An Imbalancing Act: Gap Junctions Reduce the Backward Motor Circuit Activity to Bias *C. elegans* for Forward Locomotion

Taizo Kawano,[1,6] Michelle D. Po,[1,2,6] Shangbang Gao,[1] George Leung,[3] William S. Ryu,[4,5] and Mei Zhen[1,2,*]
[1]Samuel Lunenfeld Research Institute, Mount Sinai Hospital, Toronto, ON M5G 1X5, Canada
[2]Department of Molecular Genetics, University of Toronto, Toronto, ON M5S 1A8, Canada
[3]Department of Physics, Chinese University of Hong Kong, Hong Kong, China
[4]Department of Physics, University of Toronto, Toronto, ON M5S 1A7, Canada
[5]Banting and Best Department of Medical Research, University of Toronto, Toronto, ON M5G 1L6, Canada
[6]These authors contributed equally to this work
*Correspondence: zhen@lunenfeld.ca
DOI 10.1016/j.neuron.2011.09.005

SUMMARY

A neural network can sustain and switch between different activity patterns to execute multiple behaviors. By monitoring the decision making for directional locomotion through motor circuit calcium imaging in behaving *Caenorhabditis elegans* (*C. elegans*), we reveal that *C. elegans* determines the directionality of movements by establishing an imbalanced output between the forward and backward motor circuits and that it alters directions by switching between these imbalanced states. We further demonstrate that premotor interneurons modulate endogenous motoneuron activity to establish the output imbalance. Specifically, the UNC-7 and UNC-9 innexin-dependent premotor interneuron-motoneuron coupling prevents a balanced output state that leads to movements without directionality. Moreover, they act as shunts to decrease the backward-circuit activity, establishing a persistent bias for the high forward-circuit output state that results in the inherent preference of *C. elegans* for forward locomotion. This study demonstrates that imbalanced motoneuron activity underlies directional movement and establishes gap junctions as critical modulators of the properties and outputs of neural circuits.

INTRODUCTION

The simplicity and experimental amenability of invertebrate nervous systems have helped develop critical concepts that guide our understanding of how complex neuronal networks operate (Getting, 1989; Goulding, 2009; Marder et al., 2005; Nusbaum and Beenhakker, 2002). With a fully elucidated anatomical wiring diagram (Chen et al., 2006; White et al., 1976), a large collection of genetic mutants (Brenner, 1974), and maturing tools for optical imaging and interrogation of circuit activity (Kerr et al., 2000; Leifer et al., 2011; Nagel et al., 2005; Stirman et al., 2011), *Caenorhabditis elegans* (*C. elegans*) offers an excellent model for genetic interrogation of fundamental principles that govern circuit formation and function.

C. elegans exhibits rhythmic, undulatory forward and backward locomotion (Brenner, 1974). Under standard laboratory culture conditions, *C. elegans* predominantly generates continuous forward movement that is occasionally interrupted by brief backing, with the reversal frequency modulated by sensory responses (Gray et al., 2005; Pierce-Shimomura et al., 1999). Electron microscopic reconstruction and targeted neuronal ablation of the *C. elegans* adult nervous system has led to the identification of core components of the motor circuit: five pairs of premotor interneurons, historically named as the command interneurons, receive and integrate inputs from sensory and upper layer interneurons and output upon four classes of motoneurons to generate coordinated locomotion (White et al., 1976). For directional movement, the AVA, AVE, and AVD premotor interneurons were proposed to drive or modulate backward motion through innervating the A motoneurons via both chemical and electrical synapses. The AVB and PVC premotor interneurons, on the other hand, innervate the B motoneurons exclusively through gap junctions and chemical synapses, respectively, to mediate forward motion (Chalfie et al., 1985; Wicks et al., 1996; illustrated in Figures 1A and 1B).

Despite knowing the physical connectivity of the motor circuit, mechanisms through which the *C. elegans* motor circuit selects and alters the direction of movement remain to be deciphered. The laser ablation of any single class of premotor interneurons failed to abolish movement (Chalfie et al., 1985; Wicks et al., 1996), indicating functional redundancy and modulation in such a small circuit. The ablation of AVB or AVA interneurons alone, however, led to the most prominent, albeit partial, impairment of spontaneous forward or backward movements, respectively, establishing them as the most critical regulators for directional motion (Chalfie et al., 1985; Wicks et al., 1996). Coincidentally, AVB and AVA are the premotor interneurons that form the vast majority of gap junctions with motoneurons (White et al., 1976), implying a potential involvement of gap junctions in determining directional movement. Consistently, we found that loss-of-function mutations in two innexins, the invertebrate gap junction proteins, led to altered preference and duration of *C. elegans* directional movement (see Results).

In the present study, through in vivo calcium imaging, electro-physiology, and behavioral analyses of wild-type animals and in-nexin mutants, we reveal several fundamental mechanisms for the decision-making process of directional movement by the *C. elegans* motor circuit: (1) the motor circuit establishes imbalanced forward and backward motoneuron activity states that determine the directionality of movement, and it alternates between these states to change directions; (2) premotor inter-neurons modulate endogenous motoneuron activity to establish the imbalanced motoneuron activity states; and (3) gap junctions of the backward circuit reduce the backward-circuit output, which is necessary for, and establishes the intrinsic bias toward, continuous forward movement.

RESULTS

Reciprocal Activation of Two Classes of Premotor Interneurons Correlates with Directional Movement

To address mechanisms that enable the motor circuit to execute directional movement, we established a semiautomated in vivo calcium imaging system to identify activity patterns of the *C. elegans* motor circuit associated with directional movements (see Figure S1A available online; Experimental Procedures). Briefly, late larvae (L4) or adult animals expressing a genetic calcium sensor cameleon (Miyawaki et al., 1997) in various motor circuit neurons were allowed to move and alter directions spontaneously on glass slides. Fluorescent signals from the neuron soma were tracked over time; the intensity and positional change of the fluorescent objects provided indices for neuronal activity and the direction of movement, respectively. Calcium-insensitive cameleons served as negative controls for all reporters (Figures 4 and 6; Figure S3).

We first examined the activity of AVA, AVE, and AVD pre-motor interneurons that were proposed to drive or modulate backing. Simultaneous imaging of these tightly clustered neu-rons, which was only possible in animals with restricted move-ment (Experimental Procedures), revealed temporally correlated calcium profiles for AVA and AVE, indicating their coactivation and inactivation (Figure 1C; Figure S1B; Movie S1, part A). We did not detect activity in AVD (Figure 1C), which probably reflects their proposed role in touch-stimulated, instead of spontaneous, movement (Chalfie et al., 1985; Wicks et al., 1996). To better correlate AVA and AVE activity with motion, we allowed animals to move more freely and imaged the interneuron pair as a single region of interest (ROI) (Experimental Procedures). Consistent with previous reports for AVA (Ben Arous et al., 2010; Chronis et al., 2007), the initiation of reversals (Figure 1D, dotted vertical lines) temporally correlated with a sharp increase of intracellular calcium in AVA/AVE (Figure 1D, upper trace, right). The period of gradual decline in the calcium transient correlated with continuous forward motion (Figure 1D; Movie S1, part B). Therefore, the activation of AVA/AVE is associated with backward motion.

In contrast, the initiation of forward movements (Figure 1E, dotted vertical lines) generally corresponded with a calcium increase in AVB (Figure 1E, upper trace, right), the key premotor interneuron required for spontaneous forward movement (Chal-fie et al., 1985; Wicks et al., 1996), whereas a decrease of the calcium transient correlated with either a reduced forward velocity or reversals (Figure 1E), correlating AVB activation with forward motion. We could not record PVC, premotor interneu-rons that contribute to stimulated forward motion (Chalfie et al., 1985; Wicks et al., 1996), due to the low reporter expres-sion level (data not shown).

An inverse correlation between AVA/AVE and AVB activation with the directionality of the movement of *C. elegans* implies their reciprocal activation. To test this possibility, we simultaneously imaged AVE and AVB, the only neuron pair that is spatially sepa-rated sufficiently to permit unambiguous tracking of calcium signals in animals with restricted movement. Indeed, the calcium change in AVE was anticorrelated with the calcium change in AVB (Figure 1F; Movie S1, part C). These results suggest that re-ciprocal activation and inactivation between the forward (AVB) and backward (AVA/AVE) premotor interneurons correlate with the directional movement of *C. elegans*.

Imbalanced A and B Motoneuron Output Correlates with Directional Movement

The *C. elegans* wiring diagram predicts that AVA/AVE and AVB innervate the A and B motoneurons, respectively, via chemical and/or electrical synapses (White et al., 1976). We simulta-neously imaged VB9 and VA8, two motoneurons that provide ex-citatory inputs onto adjacent ventral midposterior body muscu-lature, as a proxy for the motoneuron output of forward and backward circuits (Figure 1A).

During episodes of continuous forward and backward move-ments, VB9 and VA8 motoneurons maintained a clear separation in their calcium levels (Figures 2A and 2B; Movie S1, part D). Noticeably, a higher mean calcium level of VB9 (denoted by a red dotted line in Figure 2A) than of VA8 (denoted by a blue dotted line), referred to as the B > A state, coincided with contin-uous forward movement, whereas a higher mean activity level of VA8 than of VB9, referred to as the A > B state, coincided with backing (Figure 2A, lower trace). During continuous movement, regardless of the directionality, both VA8 and VB9 often exhibited periodic, sometimes in-phase changes over their mean calcium level (Figure 2A, asterisks), whereas VB9 and DB6 and VA8 and DA6, the same class motoneuron pairs that input onto the oppo-site ventral and dorsal musculature (Figure 1A), tend to exhibit mostly out-of-phase changes (Figure 2B, asterisks). The cause for these small calcium changes remains to be determined.

On the other hand, directional changes (Figure 2A, denoted by dotted vertical lines) coincided with the large, reciprocal switches between the mean calcium level of VA8 and VB9 or the A > B and B > A states (Figure 2A, denoted by blue and red arrows; Figure S1D). Importantly, the transition from back-ward to forward motion was temporally correlated with a calcium rise in VB9 and a calcium decrease in VA8 (Figure 2C, left), whereas reversals temporally correlated with a reversed pattern (Figure 2C, right). Critically, the initiation of a reciprocal change in the A and B motoneuron activity temporally correlates with the initiation of directional change. It is noted that the initiation of directional change generally preceded the crossover between VA8 and VB9 calcium level. The cause for this lag is unknown; one possible explanation is that because VA8/VB9 is located in the midbody, a change in directionality that has taken place in adjacent body segments contributes to the positional change
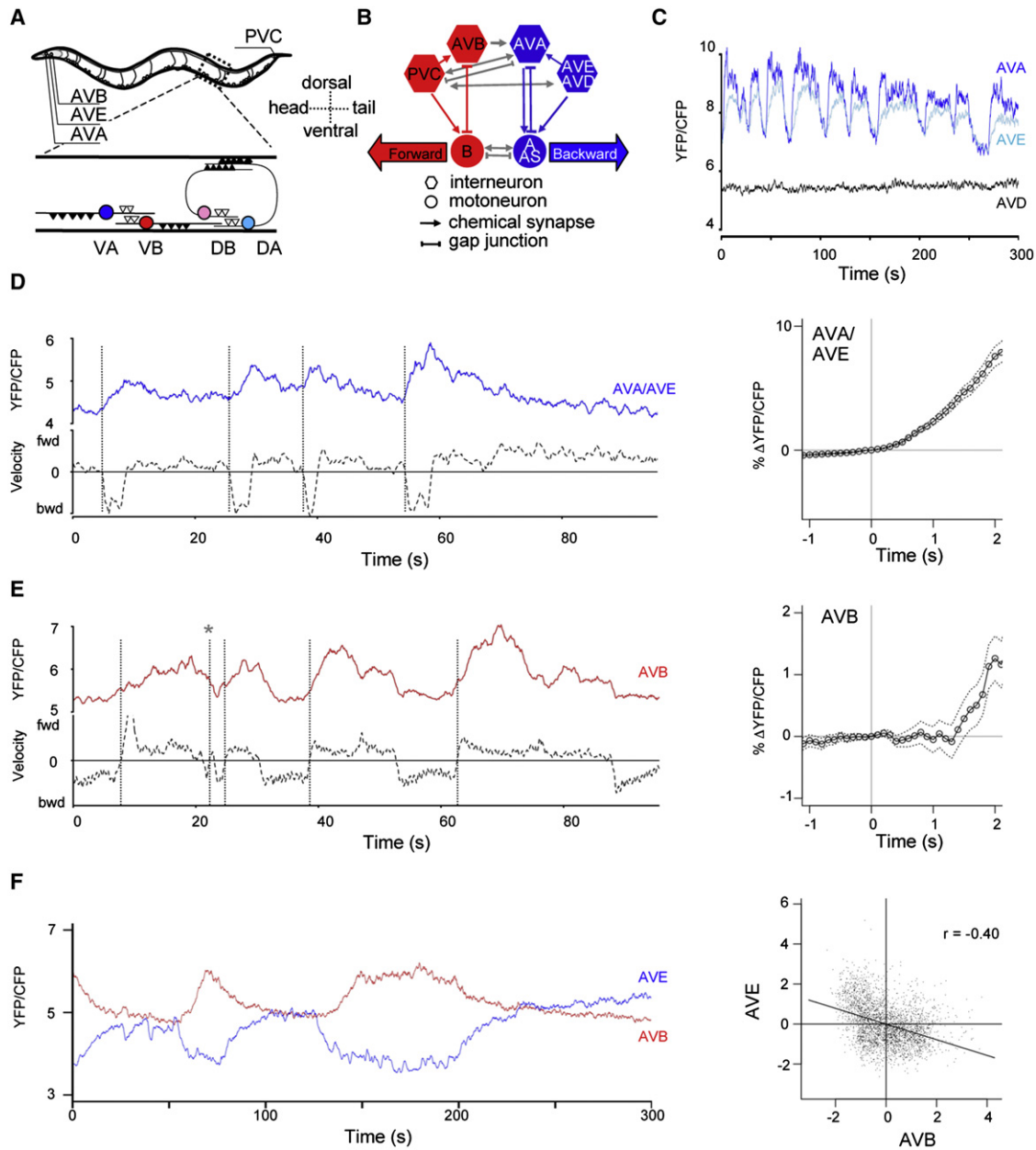
Figure 1. Reciprocal Activation of Two Classes of Premotor Interneurons during Directional Movement

(A) The anatomic organization of premotor interneurons (AVA, AVE, AVB, and PVC) and motoneurons (VA, VB, DA, and DB) that innervate ventral and dorsal musculature. VA8 and VB9 axon-dendrite organization is illustrated as synaptic input (open triangles) and output (neuromuscular junctions, solid triangles) processes.

(B) A schematic diagram of the elucidated anatomic connectivity of the *C. elegans* motor circuit (White et al., 1976). Hexagons represent premotor interneurons, circles indicate motoneurons, arrows show chemical synapses, and lines represent gap junctions. Proposed motor circuit neurons responsible for forward and backward locomotion are coded in red and blue, respectively.

(C) Simultaneous imaging of multiple premotor interneurons. Calcium transient traces for indicated neurons were shown as the YFP/CFP ratio over time by respective cameleon calcium sensors; recordings were carried out in animals with limited movements to permit unambiguous tracking of individual neurons (see Experimental Procedures). AVA and AVE, but not AVD, showed synchronized activation.

(D and E) Left: a real-time correlation of calcium transients of specific neurons (top traces) with the direction and velocity of motion (lower traces). These recordings were carried out in animals with fairly free movement to allow correlation between calcium signals and motion. The lower traces present the movement at each time point (x axis). Y axis indicates the velocity of motion in arbitrary units (a.u.). The position of each time point, above or beneath the horizontal line, represents motion in forward or backward directions, respectively.

(D) Left: the periodic rise of calcium transients in AVA/AVE (imaged as a single ROI) correlated with the initiation of backward movement (dotted vertical line, bottom trace). Right: averaged calcium transient changes (y axis) before (1 s) and after (2 s) the initiation of reversal (t = 0; x axis) exhibited a tight temporal correlation between AVA/AVE activity increase and reversal.

of the VA8/VB9 soma prior to a complete reversal of the activity level.

Together, these results indicate that the *C. elegans* motor circuit establishes and maintains an imbalanced activity between its forward (B motoneuron) and backward (A motoneuron) output module to permit directional movement. Not only do the B > A and A > B output patterns correlate with continuous forward and backward movement, respectively, but a switch between these patterns also coincides with the directional change. The preference of wild-type *C. elegans* for forward movement thus implies an inherent bias of its motor circuit to maintain B > A, the higher forward-circuit output pattern.

Two Innexin Mutants Cannot Execute Continuous Forward Movement

How does the *C. elegans* motor circuit establish an imbalanced output of A and B motoneuron activity? We examined the involvement of UNC-7 and UNC-9, two innexins expressed by the nervous system, because of the specific deficit of the respective innexin mutants in directional movements (see below).

unc-7 and *unc-9* null mutants resulted from Brenner's original *C. elegans* mutant screen (Brenner, 1974) and are characterized by a similar movement defect described as kinking: instead of generating smooth body bends, these animals assumed distorted, or "kinked," postures (Barnes and Hekimi, 1997; Brenner, 1974; Starich et al., 1993). *unc-9 unc-7* double-null mutants exhibit identical kinker behaviors, suggesting that they regulate locomotion through shared biological pathways. Previous studies revealed their roles in the coupling between AVB premotor interneurons and B motoneurons and between body wall muscles, as well as in neuromuscular junction morphology. Restoring AVB-B or muscle coupling, or neuromuscular junction morphology, in these innexin mutants, however, could not restore defective locomotion (Liu et al., 2006; Starich et al., 2009; Yeh et al., 2009).

To understand the physiological nature of their motor defects, we examined these innexin mutants by the body curvature (Pierce-Shimomura et al., 2008) and automated motion analyses (Experimental Procedures). In body curvature analyses, the forward motion is represented as body bends propagating in a head-to-tail direction (Figure 3A, black arrow) and backing is represented as body-bend propagation in a tail-to-head direction (Figure 3A, arrowheads). For motion analyses, we quantify the propensity (total percentage of time, Figure 3B) and continuity (averaged duration, Figure 3C) of directional movement.

Wild-type animals favor forward movement over backing (Figure 3A, top right; Movie S2, part A), moving both predominantly (Figure 3B) and continuously (Figure 3C) forward. *unc-7*, *unc-9*, and *unc-9 unc-7* innexin mutants reduced the overall propensity for forward movement (Figure 3B) and failed to execute continuous forward movement (Figure 3C). Instead, they generated

discontinuous short body bends (Figure 3A, asterisks in middle and lower right panels), some propagating in opposite directions along different body segments (white arrows in boxed areas), resulting in a kinked body posture (Figure 3A, left panels). Such a mode of movement, which led to no significant travel in either direction, is referred to as kinking henceforth.

Contrary to the failure in continuous forward movement, these innexin mutants propagated full tail-to-head body bends (Figure 3A, arrowheads) that led to continuous backing (Figure 3C). Moreover, in contrast to a reduced forward movement, they exhibited an increased propensity to move backward (Figure 3B; Movie S2, parts B–D). Therefore, the motor deficit of innexin mutants, a specific inability for continuous forward movement, concomitant with hyperactivated backing reflects a shift from wild-type animals' preference for forward motion to backing.

Innexin Mutants Cannot Establish B > A, the Higher Forward-Circuit Output Pattern

To identify the cause of the altered characteristics of directional motion, we examined the motoneuron output pattern in these innexin mutants. Wild-type animals generated either a B > A or an A > B pattern that is associated with continuous forward or backward movement, respectively (Figures 2A, 4A, and 4E). Strikingly, innexin mutants specifically failed to generate the B > A pattern.

During kinking, a phase in which they did not travel in either direction, VA8 and VB9 exhibited long periods of superimposed calcium transient profiles (Figures 4B, 4C, and 4E). Such a state, referred to as A = B henceforth, contrasts the case in wild-type animals in which VA8 and VB9 calcium profiles were almost always separated (Figures 2 and 4A). This indicates that kinking represents a frustrated, or nonproductive, state in which the body wall musculature receives a similar level of inputs from the A and B motoneurons to move in opposite directions.

When innexin mutants moved backward, VA8 exhibited a higher activity than that of VB9 (A > B state), with a mean difference similar to that of wild-type animals during backing (shaded areas in Figures 4B, 4C, and 4E). Therefore, although these innexin mutants were capable of generating the backing-associated, higher backward-output pattern (A > B), they failed to establish the higher forward-output pattern (B > A) that correlated with continuous forward movement in wild-type animals. It was instead replaced by B = A, an equal-output pattern that correlated with kinking.

Reestablishing the B > A Output Pattern Restores Continuous Forward Movement

If the inability of innexin mutants to execute continuous forward movement results from their inability to break an A = B output, we should be able to convert kinking into forward movement by

(E) The transition from backing to forward movement (dotted vertical lines) correlated with an increase of calcium transients in AVB (top trace). The single case in which it failed to correlate with AVB increase (dotted vertical line marked by *) probably reflected that this animal quickly switched into backing. Right: averaged calcium transient change (y axis) in AVB before and after the directional change (t = 0). AVB exhibited an increase during the initiation of reversal and forward motion, albeit with a slight delay.

(F) Left: AVE and AVB showed out-of-phase calcium transient profiles. Right: AVE and AVB activity change exhibits a significant negative correlation. Standardized data from seven recordings were subjected to correlation analysis.
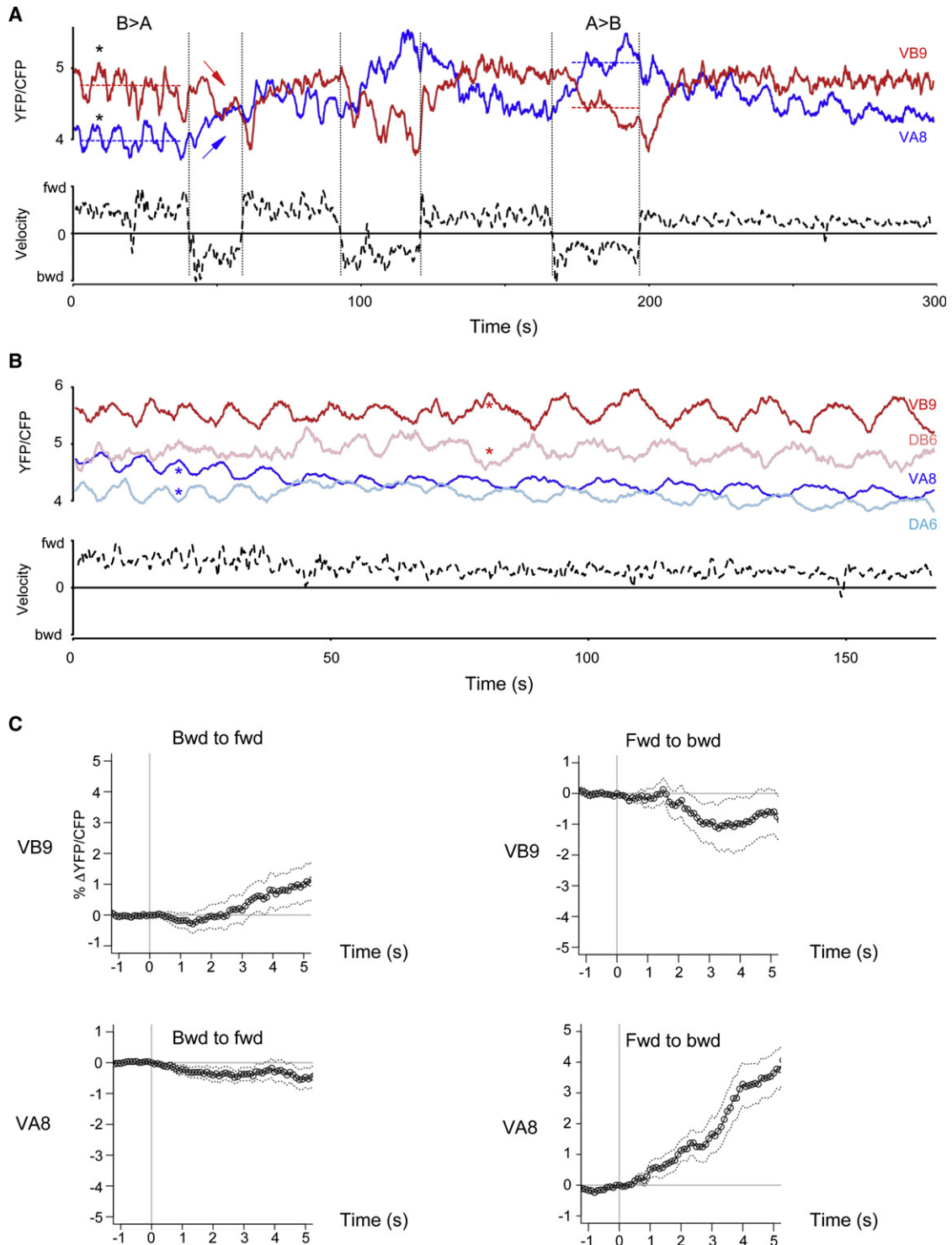
Figure 2. An Imbalanced A and B Motoneuron Activity Correlates with Directional Movement
(A and B) A real-time correlation between calcium transients of coimaged motoneuron neurons with the directionality and velocity of movement. Top: changes in cameleon signals for individual neurons (y axis) over time (x axis). Bottom: y axis indicates the velocity of motion in a.u. The position of each time point, above or beneath the horizontal line, represents motion forward or backward, respectively.
(A) A higher mean calcium transient in VA8 (blue dotted lines) or in VB9 (red dotted lines) correlated with backward or forward motion, respectively, whereas a reciprocal change of the mean activity level (red and blue arrows) correlated with directional change. Small, sometimes in-phase changes over the baseline calcium transients for VA8 and VB9 (*) occurred during continuous forward and backward movements.
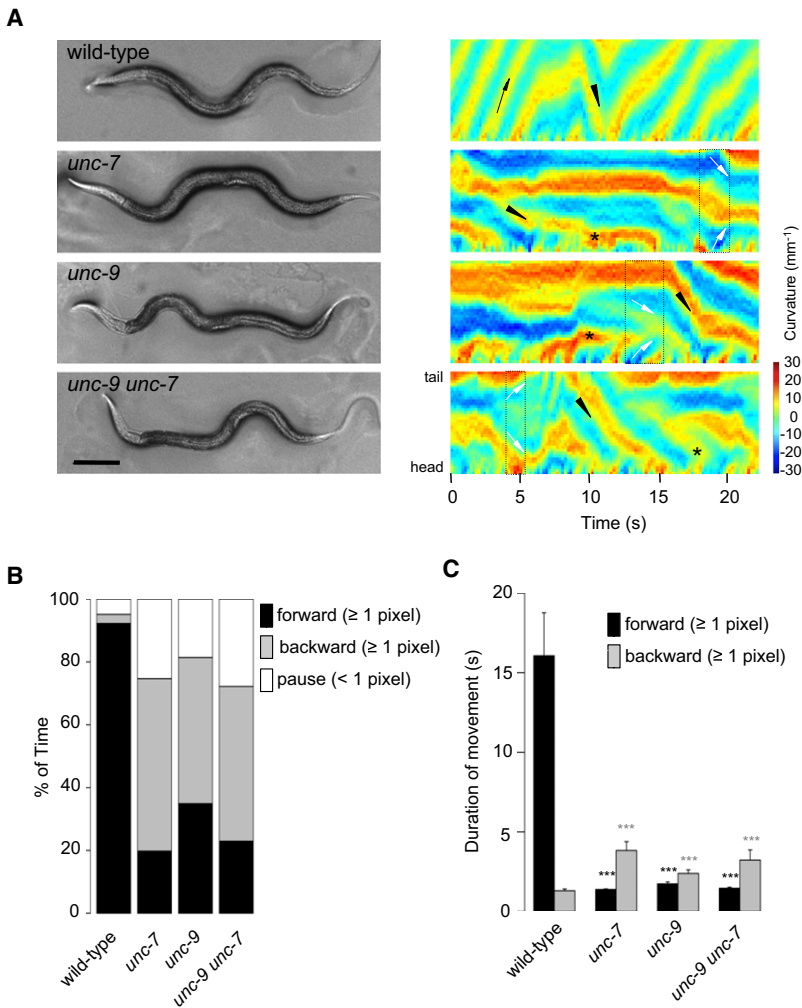
A

Figure 3. Innexin Mutants Cannot Execute Continuous Forward Movement

(A) Left: body postures of wild-type and innexin animals. Right: body curvature along the length of a moving animal of respective genotypes, as in the left panels, plotted over time. Wild-type animals exhibit primarily continuous forward motion, shown as full head-to-tail wave propagation (black arrow), with interruptions of short backing or tail-to-head propagation (arrowhead). Innexin mutants exhibit incomplete head-to-tail wave propagation and therefore no continuous forward movement (asterisks) but can coordinate backward movement (arrowheads). Examples of short body bends simultaneously propagating in opposite directions in innexin mutants are marked (white arrows in boxed areas). Scale bar represents 100 μm.

(B) The total percentage of time (video frames) animals of respective genotypes spent in forward or backward motion, or pausing. A movement of the center point of the animal ≤1 pixel between each video frame (1 fps) is defined as pausing in this study. Innexin mutants increase the propensity of backing. Time-lapse images of animals of the same genotype were pooled to generate the data set.

(C) An averaged time duration of continuous forward and backward movements for wild-type and innexin mutants. Innexin mutants exhibit reduced duration in forward motion and an increased duration in backing. n = 7, n = 12, n = 10, and n = 15 for wild-type, *unc-7*, *unc-9*, and *unc-9 unc-7* animals, respectively. ***p < 0.001 against wild-type by the Mann-Whitney U test. Error bars represent SEM.

B

C

not only correlates with, but is also necessary for, directional movement in wild-type animals. Indeed, decreasing the forward-circuit output in wild-type animals, either by reducing AVB premotor interneuron or B motoneuron activity by TWK-18(*gf*) (Experimental Procedures), led to not only a reduced forward motion but also an increased backing (Figure S2B; Movie S3, parts E and F), further supporting a causal effect of an imbalanced A and B activity during directional movement.

reestablishing the higher forward-circuit output (B > A) pattern. Indeed, when we reduced A motoneuron activity by expressing TWK-18(*gf*), a constitutively active K⁺ channel that induces membrane hyperpolarization (Kunkel et al., 2000), a B > A activity profile was reestablished (Figures 4D and 4E), accompanied by a restored continuous forward motion in these innexin mutants (Figure S2A; Movie S3, parts A–D). Behaviorally, this transgene also effectively reduced hyperactivated backing in innexin mutants (Figure S2A; Movie S3, parts A–D).

These results demonstrate that the motor deficits of these innexin mutants mainly result from their inability to establish or maintain the B > A output pattern. Moreover, they indicate that an output imbalance between the forward and backward circuits

Gap Junctions in the Backward Circuit Are Necessary for Forward Movement

UNC-7 and UNC-9 innexins are necessary for establishing the B > A pattern to execute continuous forward movement. We next investigated where each innexin is most critically required to mediate forward movement. Both innexins are broadly expressed by all premotor interneurons and motoneurons (Altun et al., 2009; Starich et al., 2009; Yeh et al., 2009). Similar to the result of a previous mosaic analysis (Starich et al., 2009), restoring the expression of wild-type UNC-7 only in AVA, one

(B) During continuous forward movement, B motoneurons (VB9 and DB6) exhibit higher calcium levels than that of A motoneurons (VA8 and DA6). The subclass of A and B motoneurons that innervate dorsal and ventral musculature (VA versus DA or VB versus DB) often show an out-of-phase change (*) over the baseline of their calcium transients.

(C) The initiation of directional change correlated with reciprocal changes of the A and B motoneuron activities. Left: the transition from backward to forward motion (t = 0) coincided with an increase in VB9 activity and a decrease in VA8 activity. Right: the transition from forward to backward motion (t = 0) coincided with an increase in VA8 activity and a decrease in VB9 activity.
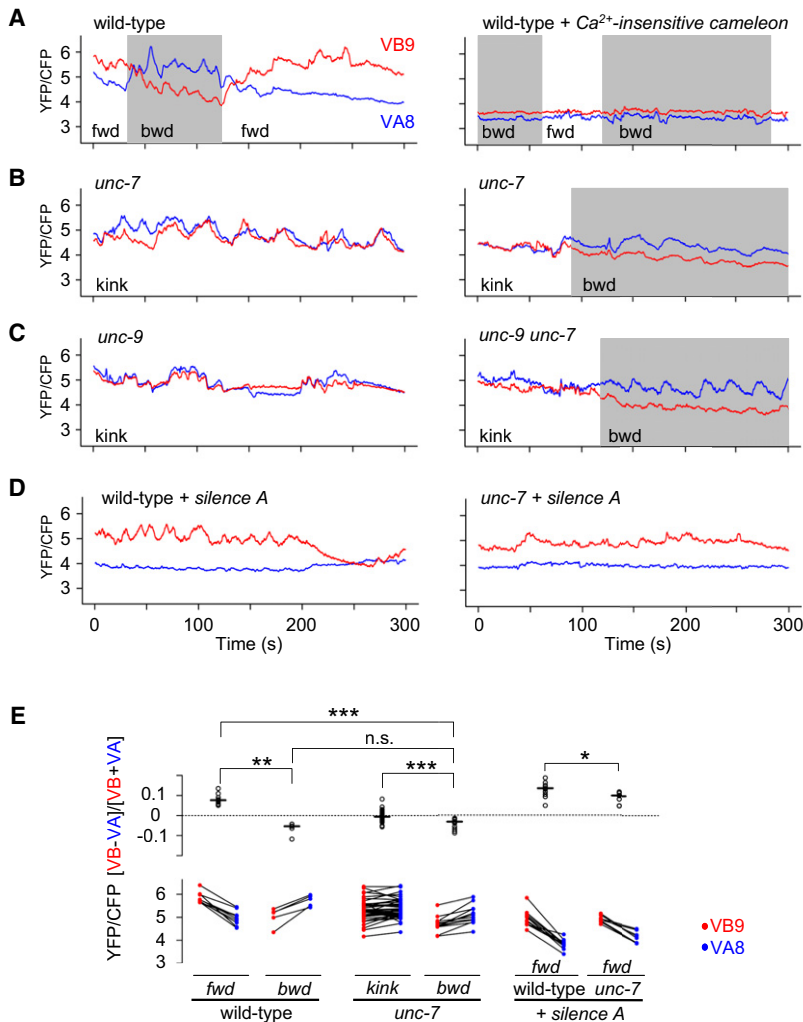
Figure 4. An Aberrant A = B Activity Pattern Prevents Forward Motion

(A–D) Representative calcium transients of VA8 (blue traces) and VB9 (red traces) motoneurons in the same animal of respective genotypes.

(A) In wild-type animals, during sustained backward movement (left, marked area), VA8 calcium transient level was higher than that of VB9. During sustained forward movement (left, unmarked areas), VB9 calcium level was higher than that of VA8.

(B and C) The kinking phase of innexin single and double mutants corresponded with a period when VA8 and VB9 exhibited similar calcium levels (unmarked areas), whereas their backward movement corresponded with a phase when the VA8 activity was higher than the VB9 activity (shaded areas).

(D) A TWK-18(gf) transgene expressed in A motoneurons effectively reduced VA8 calcium transient (blue traces) in wild-type animals (left) and unc-7 mutants (right).

(E) A quantification of the activity difference between VA8 (blue circles) and VB9 (red circles) during forward, backward, and kinking motions of wild-type and unc-7 mutants, with or without the TWK-18(gf) transgene. Measurements for VA8 and VB9 from the same animal are connected. The activity difference during the indicated phase of movement was normalized by [VB9 − VA8]/[VB9 + VA8]. n.s. indicates not statistically significant; ***p < 0.001, **p < 0.01 by the Mann-Whitney U tests.

motoneurons fasciculate. Almost every UNC-9 punctum tightly associated with a UNC-7::GFP punctum (Figure 5C). Given that AVA are the main premotor interneuron gap junction partners of A motoneurons (White et al., 1976) and that UNC-7 and UNC-9 can form heterotypic gap junctions when ectopically expressed in *Xenopus* oocytes (Starich et al., 2009), together these results strongly supports the idea that AVA-A gap junctions, mediated by UNC-7 and UNC-9, are necessary for continuous forward movement.

of the premotor interneurons of the backward circuit restored continuous forward movement in *unc-7* mutants (Figures 5A and 5B; Movie S4, parts A and B). UNC-9 was also required in the backward circuit, specifically in the A motoneurons to restore forward motion in *unc-9* mutants (Figures 5A and 5B; Movie S4, part C). Moreover, a concomitant and specific expression of UNC-7 and UNC-9 in premotor interneurons and motoneurons of the backward circuit, respectively, was necessary to restore continuous forward movement in *unc-9 unc-7* mutants (Figures 5A and 5B; Movie S4, part D). Therefore, disrupted AVA-A communication, normally mediated by UNC-7 and UNC-9, contributes significantly to the inability of *unc-7* and *unc-9* innexin mutants to travel forward.

AVA communicate with A motoneurons through both chemical and electrical synapses (Figure 1B). We examined the localization of the functionally critical innexins by immunofluorescent staining of *unc-9 unc-7* null animals coexpressing a functional UNC-7::GFP in premotor interneurons and UNC-9 in motoneurons of the backward circuit (Experimental Procedures). A punctate staining pattern of variable sizes was observed along where dendrites of these premotor interneurons and processes of

AVA-A Coupling Reduces AVA Activity to Prevent Backward Movement

How do gap junctions of the backward circuit allow and establish a bias for forward movement? In this and the next section, we show that AVA-A coupling reduces the activity of the backward circuit through two concurrent effects, both of which are required to permit the higher forward-circuit output that drives forward motion. First, AVA-A coupling reduces AVA activity to prevent hyperactivation of backing; this is supported by the following lines of evidence.

First, innexin mutants exhibit an elevated backward premotor interneuron activity via calcium imaging analyses. In innexin mutants, the level of calcium transients in AVA and AVE was significantly higher than that of wild-type animals, whether they were imaged as a single ROI (Figures 6A–6A″) or separately (Figures S3A–S3A″ and S3B–S3B″), suggesting that premotor interneurons of the backward circuit become hyperactivated in the absence of UNC-7 or UNC-9 innexins. Consistent with an
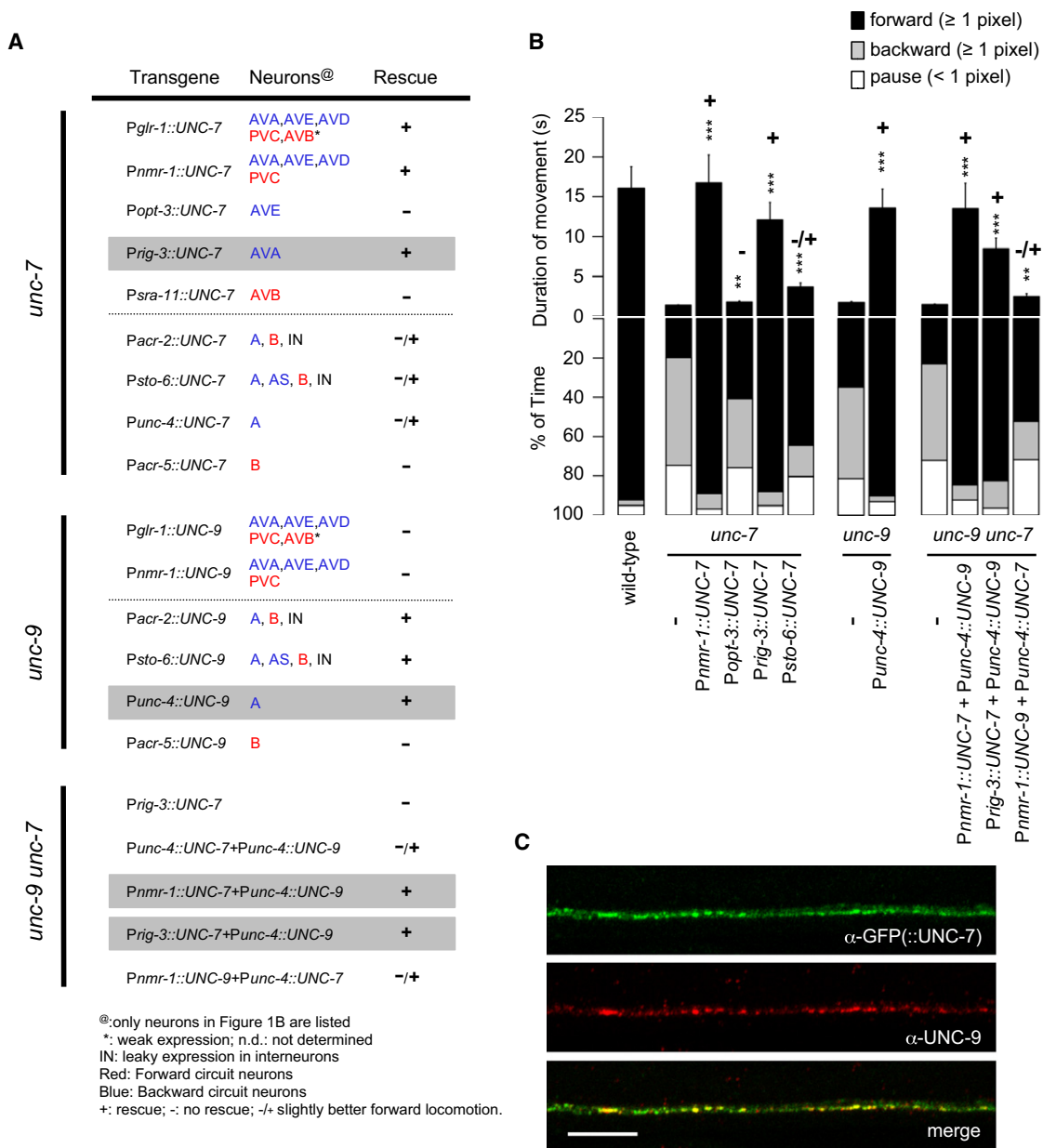
A

Transgene	Neurons@	Rescue
unc-7		
P*glr-1::UNC-7*	AVA,AVE,AVD PVC,AVB*	+
P*nmr-1::UNC-7*	AVA,AVE,AVD PVC	+
P*opt-3::UNC-7*	AVE	−
P*rig-3::UNC-7*	AVA	+
P*sra-11::UNC-7*	AVB	−
P*acr-2::UNC-7*	A, B, IN	−/+
P*sto-6::UNC-7*	A, AS, B, IN	−/+
P*unc-4::UNC-7*	A	−/+
P*acr-5::UNC-7*	B	−
unc-9		
P*glr-1::UNC-9*	AVA,AVE,AVD PVC,AVB*	−
P*nmr-1::UNC-9*	AVA,AVE,AVD PVC	−
P*acr-2::UNC-9*	A, B, IN	+
P*sto-6::UNC-9*	A, AS, B, IN	+
P*unc-4::UNC-9*	A	+
P*acr-5::UNC-9*	B	−
unc-9 unc-7		
P*rig-3::UNC-7*		−
P*unc-4::UNC-7*+P*unc-4::UNC-9*		−/+
P*nmr-1::UNC-7*+P*unc-4::UNC-9*		+
P*rig-3::UNC-7*+P*unc-4::UNC-9*		+
P*nmr-1::UNC-9*+P*unc-4::UNC-7*		−/+

@:only neurons in Figure 1B are listed
 *: weak expression; n.d.: not determined
IN: leaky expression in interneurons
Red: Forward circuit neurons
Blue: Backward circuit neurons
+: rescue; -: no rescue; -/+ slightly better forward locomotion.

B

C

Figure 5. Gap Junctions of the Backward Circuit Are Necessary for Continuous Forward Motion
(A) UNC-7 and UNC-9 are critically and differentially required in the premotor interneurons and motoneurons to restore forward movements of respective innexin mutants. Wild-type UNC-7 and/or UNC-9 cDNAs were expressed by different promoters in respective innexin null mutants indicated on the left. + and − represent the presence and absence of continuous forward motion in animals in the last larvae or adult stage; −/+ refers to a very slight improvement of forward movement. Neurons of the proposed forward and backward circuit (as illustrated in Figure 1B) are coded in red and blue, respectively.
(B) Directional movement of innexin mutants carrying various transgenes shown in (A), quantified by the duration of forward movement in seconds (top), as well as the percentage of time the animal spent in forward versus backward motion (bottom) by the motion analysis program. Data for representative full (+), minor (−/+), and no (−) rescue in transgenic innexin mutants were shown. Note that P*opt-3*-UNC-7 was scored as **−** despite leading to a change in forward duration that was statistically significant from *unc-7* (*). This is because the increase was ~0.5 s, such a small difference that was indistinguishable by eye. *** $p < 0.001$, ** $p < 0.01$ by the Mann-Whitney U tests. Error bars represent SEM.
(C) UNC-7::GFP (green) and UNC-9 (red) coexpressed in the backward premotor interneurons and A motoneurons, respectively, in *unc-9 unc-7* null mutants and colocalized along contacting ventral cord neurites. Scale bar represents 5 μm.

inverse activation between forward and backward premotor interneurons (Figure 1F), the calcium level of AVB was reduced in innexin mutants (Figures 6B–6B″). The change of cameleon

signals was not due to a change in the expression level of these calcium sensors in innexin mutants (Figure S3C). The reciprocal change in the premotor interneuron activity, specifically an
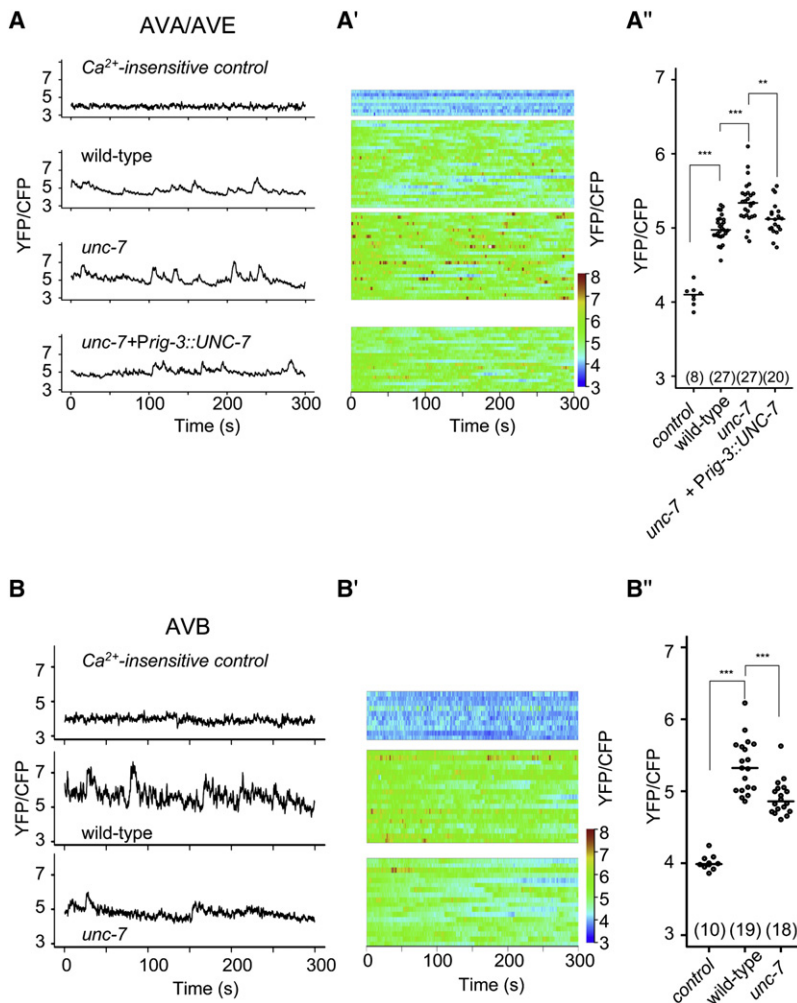
Figure 6. AVA-A Coupling Reduces AVA Activity

(A–A″) Via calcium imaging analyses, *unc-7* mutants exhibited increased AVA/AVE activity, which was reverted to wild-type level by restoring UNC-7 expression in AVA (P*rig-3::UNC-7*).

(A) Representative calcium transient traces in AVA/AVE of wild-type and innexin mutant animals recorded under identical experimental conditions.

(A′) Raster plots of calcium traces; each horizontal line corresponds to the YFP/CFP ratio of an animal of the respective genotypes, as in (A), during the 5 min recording, pseudocolored to represent calcium transient level.

(A″) Mean and distribution of the calcium transient level of each genotype. Each data point represents the averaged YFP/CFP ratio during the 5 min recording for each animal. n for each genotype is shown in parentheses.

(B–B″) AVB exhibited a decreased activity in *unc-7* mutants. $p < 0.05$, $p < 0.01$, $p < 0.001$ by the Mann-Whitney U test.

increase in AVA/AVE (backward circuit) and a decrease in AVB (forward circuit), correlates with the shift of innexin mutants' preference in directional motion to backing.

When UNC-7 expression was specifically restored in AVA in *unc-7* mutants, concurrent with restored continuous forward movement and reduced backing (Figure 5B), the calcium level in AVA/AVE was also significantly reduced (Figures 6A–6A″). However, an expression of UNC-7 in AVA of *unc-9 unc-7* mutants did not result in a rescue of forward movement (Figure 5A), implying that the reduction of AVA/AVE activity depends on restoring AVA-A coupling.

Second, AVA exhibited an increased electrical activity and increased membrane input resistance in *unc-7* mutants by in situ whole-cell recordings. AVA exhibited spontaneous excitatory electric activity (Figure 7A). The peak amplitude (Figure 7B), but not the frequency (Figure 7C), of such activities was significantly increased in *unc-7* animals; the increased amplitude was rescued when UNC-7 expression was specifically restored in AVA (Figures 7A–7C). Although there was no significant change in the resting membrane potential of AVA (Figure 7D), their input membrane resistance was significantly increased in *unc-7* mutants (Figure 7E). Such an increase was also rescued

when UNC-7 expression was restored in AVA (Figure 7E). These results indicate that UNC-7-mediated AVA-A coupling functions as shunts to dampen AVA's excitability and activity.

Third, an increased backward premotor interneuron activity contributes to the hyperactivated backing in innexin mutants. In addition to electrical coupling with AVA, A motoneurons also receive excitatory chemical synaptic inputs from AVA and AVE (Figure 1B). Hyperactivated backward premotor interneurons in innexin mutants could therefore lead to an increased chemical synaptic output to A motoneurons and contribute to their preference for backing. Indeed, when we silenced the activity of premotor interneurons of the backward circuit and PVC by P*nmr-1::TWK-18(gf)* (Figure S4), hyperactivated backing in these innexin mutants was effectively prevented (Figure S5B; Movie S5, parts B–D). Such an effect was mimicked by expressing tetanus toxin, a specific blocker of chemical synapses (Macosko et al., 2009) in the same set of premotor interneurons (Figure S5B; Movie S5, part E). Both P*nmr-1::TWK-18(gf)* (Figure S5B; Movie S5, part A) and P*nmr-1-Tetanus toxin* (Movie S5, part F) prevented continuous backing in wild-type animals. These results further support the idea that chemical synaptic output from backward premotor interneurons is required to sustain backing.

Together these results indicate that AVA-A coupling acts as shunts to dampen the activity of backward premotor interneurons in wild-type animals, which reduces their chemical synaptic inputs onto A motoneurons and prevents the hyperactivation of backing.

AVA-A Coupling Suppresses Endogenous A Motoneuron Activity to Permit Forward Movement

Reducing backward premotor interneuron activity constitutes only half of the role of AVA-A coupling in promoting forward movement. Although the AVA/AVE-silencing transgene
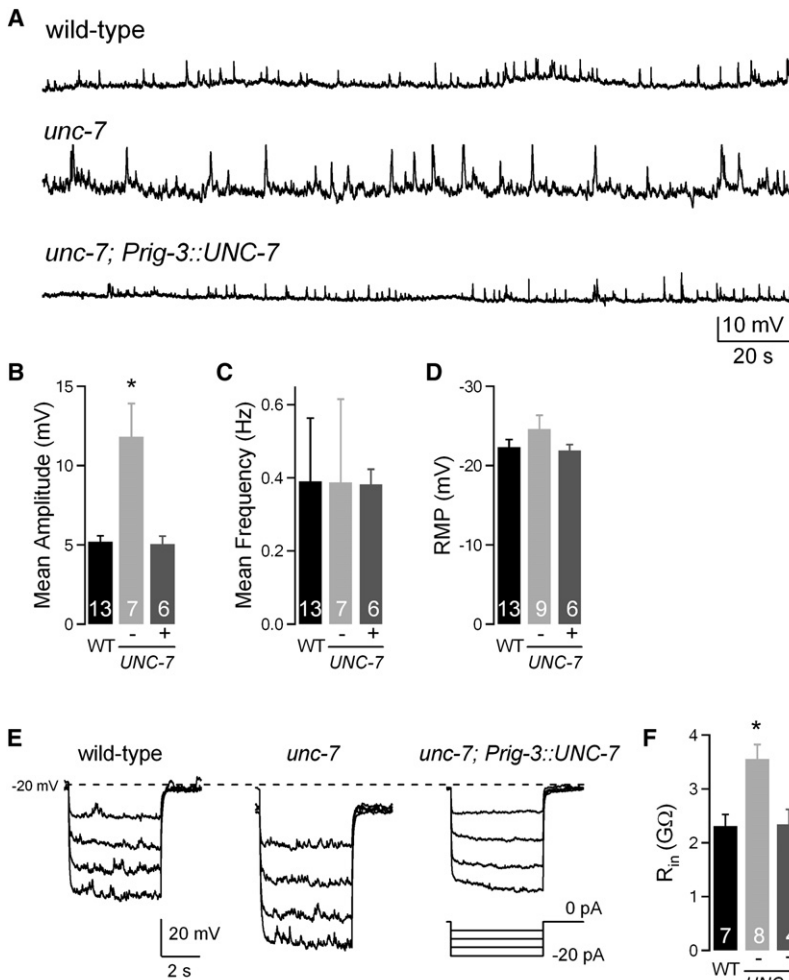
Figure 7. AVA Neurons Exhibit Increased Electric Activity and Input Resistance in *unc-7* Mutants

(A) Representative traces of spontaneous membrane potential changes in AVA neurons in wild-type animals, *unc-7(e5)* mutants, and *unc-7(e5)* expressing UNC-7 in AVA (*Prig-3::UNC-7*).

(B) The averaged peak amplitude of the spontaneous membrane potential changes was significantly increased in *unc-7* mutants and was reverted to wild-type level by restoring UNC-7 expression in AVA.

(C and D) The frequency (C) and resting membrane potential (RMP; D) were not significantly changed in *unc-7* mutants.

(E and F) Membrane input resistance (R_{in}) for AVA was increased in *unc-7* mutants.

(E) Representative traces of voltage responses to injected currents for AVA neurons in wild-type, *unc-7(e5)*, and *unc-7(e5)* animals with a restored expression of UNC-7 in AVA (*Prig-3::UNC-7*).

(F) The increased membrane input resistance in *unc-7* animals was restored by UNC-7 expression in AVA. *$p < 0.05$ against wild-type by Student's t test. Error bars represent SEM.

effectively inhibited backing in innexin mutants (Figure S5B), it did not suppress kinking: these animals still adopted a kinked posture (Figure S5A, bottom middle) instead of moving forward (Figure S5B; Movie S5, parts B–D). Consistently, although they no longer generated the backing-associated A > B pattern, they continued to establish the A = B pattern (Figures 8A–8A″). This contrasted the case in wild-type background, in which inactivating AVA/AVE by the same transgene led to an exclusive B > A pattern (Figures 8A–8A″) and forward movement (Figures S5A and S5B; Movie S5, part A).

The failure to further reduce A activity when AVA were silenced (Figures 8A–8A″; Figure S4) is consistent with the notion that AVA and A are uncoupled in these innexin mutants. However, observing a persistent A motoneuron activity in the presence of this transgene was unexpected because silencing AVA and AVE eliminates both chemical and electrical synaptic inputs to A motoneurons (Figure 1B). The residual A motoneuron activity may therefore represent a premotor interneuron-independent (referred to as endogenous) motoneuron activity that is suppressed by their coupling with AVA to allow the establishment of a B > A output pattern in wild-type animals. Alternatively, because transient cell coupling may be necessary for circuit

maturation, a persistent A motoneuron activity could reflect the consequence of miswiring in these innexin mutants in that they receive aberrant inputs from other premotor interneurons.

To distinguish between these possibilities, we used TWK-18(*gf*) to reduce the activity of all premotor interneurons (Experimental Procedures). In the wild-type background, this transgene led to prolonged pausing in a straight body posture (Figure S5A, top right), coinciding with reduced VB9 and VA8 activity (Figures 8B–8B″). Sluggish forward motion was occasionally observed in these animals (Movie S6, part A), probably due to an incomplete silencing of the forward-circuit activity. Innexin mutants expressing the same transgene, however, continued kinking (Figure S5A, bottom right; Movie S6, parts B–D), failed to execute continuous forward movement (Figure S5B), and only generated an A = B pattern (Figures 8B–8B″). Therefore, the residual VA8 activity reflects an endogenous A motoneuron activity that is normally suppressed by AVA-A coupling. The suppression of this endogenous activity is necessary for wild-type animals to establish a B > A pattern and to execute continuous forward movement.

Taken together, gap junctions in the backward circuit suppress the activity of both backward premotor interneurons and A motoneurons, maintaining the backward circuit at a low output state and promoting continuous forward movement.

Premotor Interneurons Modify Endogenous Motoneuron Activities to Establish Imbalanced Motoneuron Outputs

Silencing all premotor interneuron inputs still failed to suppress kinking or to alter the A = B output pattern in innexin mutants. This suggests that in innexin mutants, not only A but also B motoneurons are uncoupled from premotor interneurons, and they exhibit an equal output of a premotor interneuron-independent,
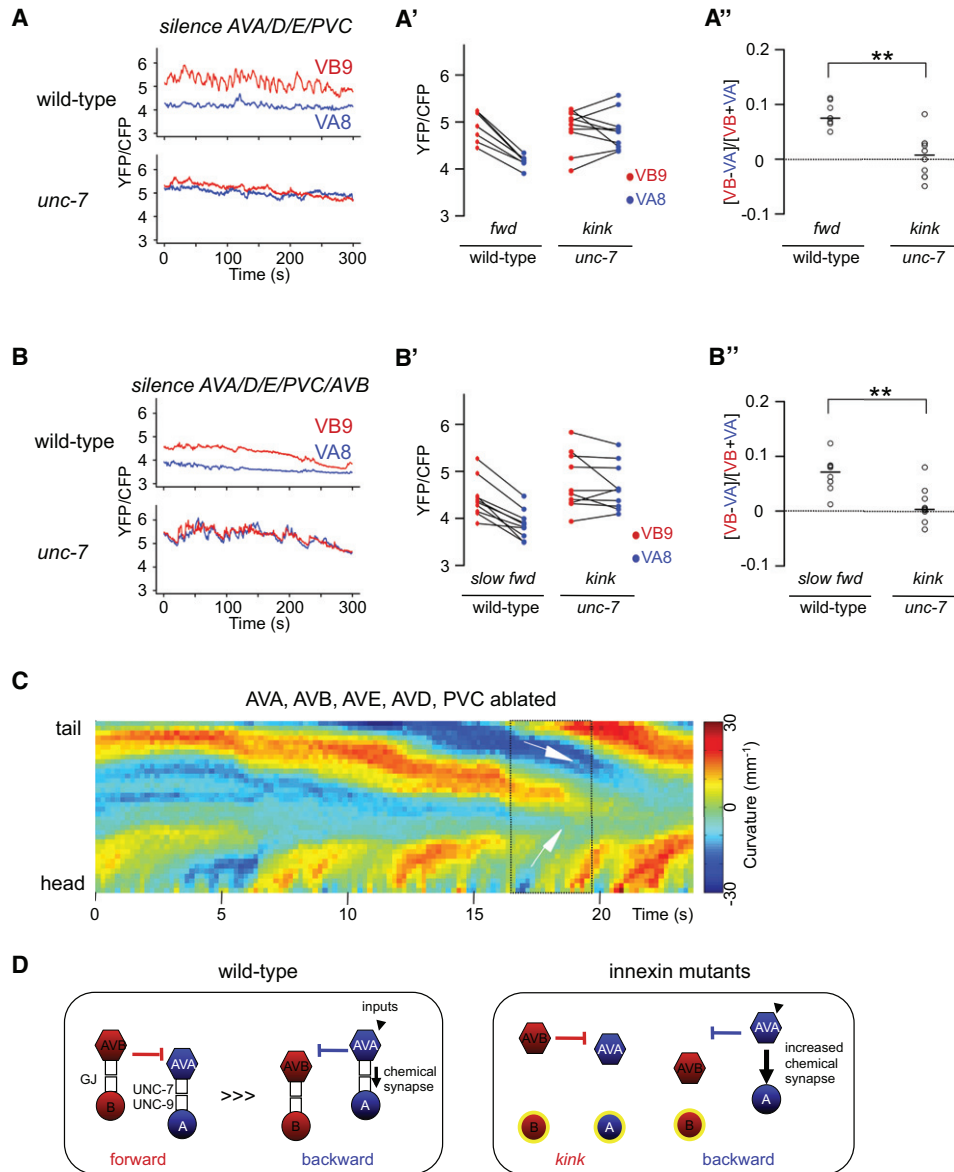
Figure 8. AVA-A Coupling Suppresses an Endogenous A Activity to Permit Forward Motion

(A–A″) Reducing backward premotor interneuron activity did not rescue kinking.

(A) Representative motoneuron calcium traces of wild-type (top) and *unc-7* (bottom) animals that expressed silencer transgene *TWK-18(gf)* in backward circuit premotor interneurons and PVC.

(A′ and A″) A quantification of the differential activity between VA8 and VB9.

(B–B″) Reducing all premotor interneuron activity did not rescue kinking. Representative traces (B) and quantification (B′ and B″) show VA8 and VB9 activity when all premotor interneurons were inactivated by TWK-18(gf) silencer in wild-type and *unc-7* mutants. Red dots represent the mean VB9 activity of an animal during the indicated mode of movement; the connected blue dots represent VA8 activity during the same period of movement; fwd indicates forward motion; kink indicates kinking. The mean activity difference was normalized by [VB9 − VA8]/[VB9 + VA8]. ***$p < 0.001$; **$p < 0.01$; *$p < 0.05$; n.s. by the Mann-Whitney U test.

(C) The body curvature of a wild-type adult with all premotor interneurons physically removed. It exhibited kinked posture characterized by discontinuous and opposing body bends (white arrows).

(D) A model for how the *C. elegans* motor circuit regulates directional movement. Higher positions represent higher activity states of premotor interneurons and motoneurons. Cylinders represent gap junction (GJ); arrows indicate chemical synapse; arrowheads show depolarizing signal; colored lines represent reciprocal inhibition; >>> indicates that the diagram on the left is a preferred state; yellow circles show endogenous activity. Left: UNC-7-UNC-9-mediated GJs between premotor interneurons and motoneurons facilitate the establishment and transitions between the B > A and A > B states that drive forward or backward movements, with B > A being the preferred state. Right: in the absence of these couplings, the motor circuit exhibits either the B = A state that results from motoneurons' endogenous activity and leads to kinking or an A > B state that results from an increased activity and chemical synaptic output of AVA, which leads to hyperactivated backing.

endogenous motoneuron activity that contributes to kinking. All direct inputs from AVB to B motoneurons are gap junctions (Figure 1B); therefore, both forward and backward premotor interneurons employ gap junctions to suppress or modify the endogenous motoneuron activity to prevent their output equilibrium.

If the endogenous motoneuron activity observed in innexin mutants reflects a state of the wild-type motoneurons when they become uncoupled from the motor circuit, the physical removal of premotor interneurons in wild-type animals should reveal such a state and recapitulate kinking. Indeed, when all premotor interneurons were ablated in wild-type animals (Figure S6; Experimental Procedures), they generated discontinuous short body bends characteristic of kinking (Figure 8C; Movie S7). This contrasts the consequence of hyperpolarizing all premotor interneurons by TWK-18(*gf*) in wild-type animals, which could effectively reduce motoneuron activity through gap junctions, hence preventing body bends (Figure S5A, top right; Movie S6, part A). Therefore both A and B motoneurons exhibit activities in the absence of premotor interneuron inputs; their coupling with premotor interneurons is necessary for a separation of their activity level, which prevents kinking and underlies directional movement.

DISCUSSION

A Model for Decision Making in Directional Movement
In this study, we show that an imbalanced activity of B and A motoneurons, the output modules of the forward and backward circuits, underlies the directionality of *C. elegans* movement (Figure 8D). We demonstrate that gap junctions between premotor interneurons and motoneurons (GJ, illustrated as cylinders in Figure 8D) are necessary for establishing an imbalanced motoneuron output. In the absence of these couplings, an endogenous A and B motoneuron activity (yellow circles in Figure 8D) leads to an equal motoneuron output and nondirectional movement (kinking). We propose that the reciprocal activation of premotor interneurons of the forward and backward circuit (colored lines in Figure 8D) leads to the establishment and the switching between the A > B and B > A patterns through modifying the endogenous B and A motoneuron activity.

We further demonstrate that UNC-7-UNC-9-mediated gap junctions in the backward circuit maintain the backward circuit at a low state by suppressing the activity of both AVA premotor interneurons and A motoneurons. They establish the intrinsic bias (>>> in Figure 8D) for a higher forward-circuit output (B > A) and are necessary for continuous forward movement. Such a bias ensures that only upon strong backward-premotor interneuron activation (input, illustrated as arrowheads in Figure 8D) is an A > B pattern established via the increased chemical (arrows in Figure 8D) and electrical synaptic inputs to A motoneurons to permit brief backing.

An Analogous Operation between *C. elegans* and Other Motor Circuits
Our studies indicate that an endogenous activity of the *C. elegans* motoneurons is modulated by premotor interneurons to exhibit different output levels. It supports a notion that premotor interneurons of the forward and backward circuits function as

organizers to establish the differential output pattern between distinct motoneuron pools. Such an operational model bears intriguing resemblance to that of other motor systems. For example, mouse spinal cord premotor interneurons act as organizers of the oscillating motoneuron activity to establish an alternate, left-right firing pattern that permits walking and prevents hopping of the hind limbs (Crone et al., 2008; Lanuza et al., 2004; Zhang et al., 2008). Critically, in both motor systems, inputs from specific interneuron pools are necessary to break the equilibrium of an otherwise synchronized motor output pattern.

Remaining Questions for Decision Making in Directional Movement
This study mainly focused on the role of premotor interneuron-motoneuron coupling in the backward circuit in directional movement; questions remain regarding how other circuit components contribute to such a decision-making process.

How premotor interneurons of the forward circuit instruct directional motion remains elusive. UNC-7 and UNC-9 innexins mediate heterotypic gap junctions between AVB and B motoneurons (Starich et al., 2009). Restoring their expression in the forward circuit, however, did not rescue forward movement in respective innexin mutants (Figure 5A; discussion in Starich et al., 2009), whereas restoring AVA-A coupling resulted in a robust rescue (Figures 5A and 5B). This implies either that the electrical coupling in the forward circuit plays a modulatory but less essential role (compared to those of the backward circuit) for forward movement or that in these innexin mutants, the communication between AVB and B is partially retained through AVB-mediated but indirect synaptic inputs onto B. How AVB-B coupling modulates B activity during directional movement remains to be better defined. Moreover, how PVC, premotor interneurons with chemical synaptic inputs onto B, contribute to forward movement should also be addressed in future studies.

This model predicts that the reciprocal activation of the forward and backward premotor interneurons establishes an imbalanced motoneuron output. Cross-inhibition between the *C. elegans* forward and backward circuit was proposed to underlie directional movement (Wicks et al., 1996; Zheng et al., 1999). We observed an anticorrelation between the activation for the forward and backward premotor interneurons, providing the first direct evidence for such a mechanism. How AVA/AVE and AVB cross-inhibition is established remains to be resolved. Although AVA receive direct synaptic inputs from AVB, AVA have no direct synaptic inputs to AVB (White et al., 1976). RIM, an interneuron that forms gap junctions with AVA and has synaptic inputs to AVB, was proposed to inhibit AVB activity through releasing tyramine (Alkema et al., 2005; Pirri et al., 2009). Supporting the notion that AVA activate RIM via gap junctions to inhibit AVB, RIM exhibited coactivated calcium transients as AVA/AVE (Figure S1C).

Gap Junctions Negatively Regulate Circuit Output
AVA-A coupling establishes a circuit bias for forward movement, highlighting a role for gap junctions in affecting circuit properties and outputs. Recent studies have begun to reveal more

sophisticated effects that gap junctions exert on coupled neurons and neural networks than simply ensuring their synchrony (Rela and Szczupak, 2004).

In the *C. elegans* motor circuit, AVA-A coupling leads to a decreased input membrane resistance in AVA, resulting in a reduced backward-premotor interneuron activity. Such an outcome resembles a cell coupling-mediated shunting effect that alters neuron and circuit output: when current flows from a more positive cell to a more negative cell, the first cell becomes less depolarized (Bennett and Zukin, 2004). These gap junctions allow motoneurons' feedback on premotor interneurons to create the appropriate motor pattern.

Gap junctions between AVA and A result in a reduced A moto-neuron output through multiple mechanisms: (1) by shunting AVA activity, these gap junctions decrease the chemical synaptic inputs to A; (2) AVA-A coupling dampens the endogenous A activity, probably also through shunting; and (3) an asymmetric property of heterotypic gap junctions could further assist AVA in maintaining A motoneurons at a low state through couplings.

Asymmetric electrical synapses occur when neurons of distinct membrane properties are coupled (Giaume and Korn, 1983) and/or when coupling is mediated by heterotypic gap junctions (Phelan et al., 2008). Indeed, UNC-7-UNC-9 heterotypic gap junctions exhibit some asymmetric gating properties in *Xenopus* oocytes (Starich et al., 2009). Moreover, in wild-type animals, hyperpolarizing AVA and AVE led to an effective reduction of A motoneuron activity (Figure 8A); by contrast, hyperpolarizing A motoneurons, although they prevented animals from backing (Movie S3, parts B–D), failed to reduce AVA activity (Figure S7), supporting an instructive role of AVA on A. It is plausible that through both cell coupling-mediated shunting on AVA and A and an asymmetric junctional property that favors AVA to A communication, gap junctions between AVA and A maintain the backward circuit at a low activity state, enabling a bias for higher forward-circuit output and continuous forward movement.

In summary, gap junctions play a critical role in *C. elegans* directional motion. Instead of being static connecting modules, they alter the activity of coupled neurons, tip the output balance between the forward and backward circuit, and establish the intrinsic properties and output bias of the *C. elegans* motor circuit. Gap junctions may serve similar regulatory roles in other neural networks, given their presence in most mature nervous systems.

EXPERIMENTAL PROCEDURES

Strains and Constructs

Standard methods were used for culturing and handling animals on Nematode Growth Medium plates (Brenner, 1974). *unc-7(e5)*, *unc-9(fc16)*, and *unc-9 (fc16) unc-7(e5)* null mutants were used throughout the study. Interneuron cameleon reporter lines *hpIs157*, *hpIs179*, and *hpIs190* were generated as follows: pJH1579, pJH1973, and pJH1969 were individually coinjected with a *lin-15* rescuing plasmid into *lin-15(n765)*, integrated into the *C. elegans* genome, and outcrossed four to six times against the N2 strain. pJH1863 was coinjected with a *lin-15* marker into *lin-15(n765)* to generate the transgenic array *hpEx1911*. *hpEx1911* was crossed into *unc-7(e5) lin-15(n765)*, integrated, and outcrossed three times to generate the motoneuron cameleon reporter *hpIs171*. Neuronal subtype promoter-driven expression of UNC-7, UNC-9, TWK-18(*gf*), and Tetanus Toxin constructs were coinjected with

dpy-20(+) or P*odr-1::GFP* injection marker in *unc-7*, *unc-9*, and *unc-9 unc-7* mutants with or without the *dpy-20(e1218)* background to generate respective transgenic animals. The transgenic arrays for TWK-18(*gf*) were outcrossed against the N2 strain from *unc-7*, *unc-9*, and *unc-9 unc-7* backgrounds as controls for their effects in innexin mutants. *akIs11* was obtained from A.V. Maricq (University of Utah) and crossed into *hpIs179* and *hpIs190* for neuronal ablation studies. A list of constructs and transgenes generated for this study is provided in Supplemental Experimental Procedures.

Calcium Imaging
Microscope Setup

Images were captured on a Zeiss Axioskop 2 Plus equipped with a motorized stage (ASI MS-4000), a dual-view beam splitter (Photometrics, Tucson, AZ) and a Charge-Coupled Device camera (Hamamatsu Orca-R2). The excitation light, derived from X-Cite (EXFO Photonic Solutions, Mississauga, ON, Canada), was reduced to about 1% by iris of the light source and Neutral Density filter. The fluorescent images were split by dual-view with a CFP/YFP filter set and projected onto the CCD camera operated by Velocity (Improvision, Lexington, MA) or MicroManager (http://micro-manager.org). The 4×-binned images were obtained at 50–100 ms exposures, 10–20 fps for 5 min. The YFP and CFP fluorescent intensities were measured by in-house-developed ImageJ plugins (http://rsb.info.nih.gov/ij).

Automated Tracking System and Motion Analysis

Calcium imaging experiments were performed either by manually recentering moving animals on the stage or through an in-house-developed acquisition software that controls the camera and motorized stage through Micromanager and ImageJ. Each frame of the acquired images was subjected to real-time processing to detect targeted cells, track objects, record stage positions, and recenter the tracked object. During postimaging processing, two regions of interest were set to detect the anterior-posterior axis. VA8 and DB6 were used as anterior and posterior cells, respectively, in motoneuron imaging. AVA/AVE or AVB and cluster of cells were used in interneuron imaging. The cell position at each time point was determined based on the coordinates of the stage position and cell position in the field of view, and the velocity was calculated by changes in the cell position between each frame. The forward and backward directions were determined by comparing changes in the anterior-posterior axis.

Interneuron Imaging

Interneuron imaging was performed under two different conditions.

(1) Imaging when animals were allowed relatively free movement (Figures 1D, 1E, and 6). This condition allows correlation between motion and changes in calcium signals. Animals were placed on freshly made 2% wet agarose pads, mounted with a few microliters of M9 buffer, and imaged with a 16× objective through the automated tracking system. We imaged multiple interneurons as a single ROI in the head region of *hpIs190* (AVA and AVE) or a single interneuron as an ROI in *hpIs179* (AVB).

(2) Imaging when animals were allowed restricted movement. Single-neuron imaging of AVA or AVE with *hpIs157* and *hpIs190* (Figure 1C; Figures S1B, S1C, S3, and S7), and AVB and AVE simultaneous imaging in a strain carrying both *hpIs157* and *hpIs179* (Figure 1F), was carried out under this condition. In both *hpIs157* and *hpIs190*, the closely spaced cell bodies prevented precise tracking at individual neuron resolution when animals were allowed free movement. Animals were mounted on dried 5% agarose pads with a few microliters of M9 buffer, covered by a coverslip, and imaged with a 63× objective. Under this condition, the movement of animals was restricted to allow the separation and tracking of signals from individual neurons, and we observed that all four head neurons, AVA, AVE, RIM, and AVD, in the *hpIs190* (P*nmr-1::D3cpv*) strain showed synchronized calcium transients, except for AVD, which had no obvious change of calcium transient profile (Figure 1C). The YFP/CFP ratio showed correlation with the relatively large movement under this recording condition (data not shown). AVE and AVB coimaged showed out-of-phase profiles and negative correlation (Figure 1F). The YFP/CFP value for AVE and AVB recording in each sample was normalized by mean and SD. Pearson's correlation coefficient was determined by R. Under this recording condition, backward motion was hyperstimulated compared to standard culturing conditions.

Interneuron Calcium Signal Analysis

For correlation analyses of the averaged YFP/CFP ratio change during transitions of directions, YFP/CFP ratios before and after directional change were collected and normalized against the YFP/CFP value immediately before the directional change. Traces from nine AVA/AVE and 15 AVB recordings were used for correlation analysis in Figures 1D and 1E. For correlation analysis between AVE and AVB activity, seven AVE/AVB recordings were analyzed to obtain the data shown in Figure 1F.

To compare the interneuron calcium signals between wild-type and innexin mutant animals, we compared the averaged YFP/CFP ratio instead of ΔR/R. YFP/CFP ratio for each sample during 5 min was presented by raster plots. The averaged YFP/CFP value over 5 min of recording for each sample was considered a single data point and presented as scatter plots (Figure 6; Figures S3A, S3B, and S7). This is because neurons analyzed in this study showed relatively high-frequency activation, and we rarely observed the decline of the calcium level to the basal value. In this case, measuring ΔR/R probably leads to an inaccurate measurement of neuronal activity.

Motoneuron Imaging

Imaging of motoneurons was carried out with a protocol modified from the AVA and AVE single-neuron imaging method (Figures 2, 4, and 8; Figure S1D). We dropped 20 μl M9 buffer onto a 2% dried agarose pad, and ~20 adult animals were placed in the liquid as spacers. Ten last-larval stage (L4) hpIs171 animals were placed in the buffer, covered by a coverslip, and imaged with a 63× objective. Neurons were identified by their stereotypic anatomical organization.

Most data presented in Figures 4 and 8 were obtained by manually recentering the moving animals during the recording and scoring the forward, backward, and kinking motion manually based on the direction of the body-bend propagation. During later parts of the study, we utilized an in-house-developed automated tracking software to recenter animals, which allowed the automated analysis of the directional movement, as well as correlation between calcium transients with directions and velocity (Figures 2A and 2B, bottom). Samples that show sustained forward or backward movement (Figures 4 and 8), instead of frequent directional change (Figure S1D), were quantified for the mean calcium level in continuous directional movement (Figures 4 and 8). Locomotion direction and calcium transients showed similar correlation pattern in both data sets.

Motoneuron Calcium Signal Analysis

Periods of backward, forward, and kinking were scored for each imaged sample. The mean of YFP/CFP ratios for VA8 and VB9 during these periods was considered the averaged activity for VA8 and VB9 for each animal during the indicated mode of locomotion. The difference between the VB9 and VA8 activity level in each animal was normalized by [VB9 − VA8]/[VB9 + VA8]. For correlation analysis, VA8 and VB9 transients of each sample were corrected for photobleaching by dividing fitted linear regression line, normalized by mean and SD. For correlation analyses of VA8 and VB9 activity change during the transition of directions, eight VA8/VB9 imaging traces were used for correlation analyses. Pearson's correlation coefficient was calculated by R.

Other Experiments

Detailed procedures for curvature analysis, automated movement analysis, electrophysiology, molecular biology, neuron silencing, ablation and chemical synapse inactivation, immunofluorescent staining, and statistical analysis are provided in Supplemental Experimental Procedures.

SUPPLEMENTAL INFORMATION

Supplemental Information includes seven figures, Supplemental Experimental Procedures, and seven movies and can be found with this article online at doi:10.1016/j.neuron.2011.09.005.

REFERENCES

Alkema, M.J., Hunter-Ensor, M., Ringstad, N., and Horvitz, H.R. (2005). Tyramine Functions independently of octopamine in the Caenorhabditis elegans nervous system. Neuron 46, 247–260.

Altun, Z.F., Chen, B., Wang, Z.W., and Hall, D.H. (2009). High resolution map of Caenorhabditis elegans gap junction proteins. Dev. Dyn. 238, 1936–1950.

Barnes, T.M., and Hekimi, S. (1997). The Caenorhabditis elegans avermectin resistance and anesthetic response gene unc-9 encodes a member of a protein family implicated in electrical coupling of excitable cells. J. Neurochem. 69, 2251–2260.

Ben Arous, J., Tanizawa, Y., Rabinowitch, I., Chatenay, D., and Schafer, W.R. (2010). Automated imaging of neuronal activity in freely behaving Caenorhabditis elegans. J. Neuroscience Methods 187, 229–234.

Bennett, M.V., and Zukin, R.S. (2004). Electrical coupling and neuronal synchronization in the Mammalian brain. Neuron 41, 495–511.

Brenner, S. (1974). The genetics of Caenorhabditis elegans. Genetics 77, 71–94.

Chalfie, M., Sulston, J.E., White, J.G., Southgate, E., Thomson, J.N., and Brenner, S. (1985). The neural circuit for touch sensitivity in Caenorhabditis elegans. J. Neurosci. 5, 956–964.

Chen, B.L., Hall, D.H., and Chklovskii, D.B. (2006). Wiring optimization can relate neuronal structure and function. Proc. Natl. Acad. Sci. USA 103, 4723–4728.

Chronis, N., Zimmer, M., and Bargmann, C.I. (2007). Microfluidics for in vivo imaging of neuronal and behavioral activity in Caenorhabditis elegans. Nat Methods 4, 727–731.

Crone, S.A., Quinlan, K.A., Zagoraiou, L., Droho, S., Restrepo, C.E., Lundfald, L., Endo, T., Setlak, J., Jessell, T.M., Kiehn, O., and Sharma, K. (2008). Genetic ablation of V2a ipsilateral interneurons disrupts left-right locomotor coordination in mammalian spinal cord. Neuron 60, 70–83.

Getting, P.A. (1989). Emerging principles governing the operation of neural networks. Annu. Rev. Neurosci. 12, 185–204.

Giaume, C., and Korn, H. (1983). Bidirectional transmission at the rectifying electrotonic synapse: a voltage-dependent process. Science 220, 84–87.

Goulding, M. (2009). Circuits controlling vertebrate locomotion: moving in a new direction. Nat. Rev. Neurosci. 10, 507–518.

Gray, J.M., Hill, J.J., and Bargmann, C.I. (2005). A circuit for navigation in Caenorhabditis elegans. Proc. Natl. Acad. Sci. USA 102, 3184–3191.

Kerr, R., Lev-Ram, V., Baird, G., Vincent, P., Tsien, R.Y., and Schafer, W.R. (2000). Optical imaging of calcium transients in neurons and pharyngeal muscle of C. elegans. Neuron 26, 583–594.

Kunkel, M.T., Johnstone, D.B., Thomas, J.H., and Salkoff, L. (2000). Mutants of a temperature-sensitive two-P domain potassium channel. J. Neurosci. 20, 7517–7524.

Lanuza, G.M., Gosgnach, S., Pierani, A., Jessell, T.M., and Goulding, M. (2004). Genetic identification of spinal interneurons that coordinate left-right locomotor activity necessary for walking movements. Neuron 42, 375–386.

Leifer, A.M., Fang-Yen, C., Gershow, M., Alkema, M.J., and Samuel, A.D. (2011). Optogenetic manipulation of neural activity in freely moving Caenorhabditis elegans. Nat. Methods 8, 147–152.

Liu, Q., Chen, B., Gaier, E., Joshi, J., and Wang, Z.W. (2006). Low conductance gap junctions mediate specific electrical coupling in body-wall muscle cells of Caenorhabditis elegans. J. Biol. Chem. 281, 7881–7889.

Macosko, E.Z., Pokala, N., Feinberg, E.H., Chalasani, S.H., Butcher, R.A., Clardy, J., and Bargmann, C.I. (2009). A hub-and-spoke circuit drives pheromone attraction and social behaviour in *C. elegans*. Nature *458*, 1171–1175.

Marder, E., Bucher, D., Schulz, D.J., and Taylor, A.L. (2005). Invertebrate central pattern generation moves along. Curr. Biol. *15*, R685–R699.

Miyawaki, A., Llopis, J., Heim, R., McCaffery, J.M., Adams, J.A., Ikura, M., and Tsien, R.Y. (1997). Fluorescent indicators for Ca2+ based on green fluorescent proteins and calmodulin. Nature *388*, 882–887.

Nagel, G., Brauner, M., Liewald, J.F., Adeishvili, N., Bamberg, E., and Gottschalk, A. (2005). Light activation of channelrhodopsin-2 in excitable cells of *Caenorhabditis elegans* triggers rapid behavioral responses. Curr. Biol. *15*, 2279–2284.

Nusbaum, M.P., and Beenhakker, M.P. (2002). A small-systems approach to motor pattern generation. Nature *417*, 343–350.

Phelan, P., Goulding, L.A., Tam, J.L., Allen, M.J., Dawber, R.J., Davies, J.A., and Bacon, J.P. (2008). Molecular mechanism of rectification at identified electrical synapses in the Drosophila giant fiber system. Curr. Biol. *18*, 1955–1960.

Pierce-Shimomura, J.T., Morse, T.M., and Lockery, S.R. (1999). The fundamental role of pirouettes in *Caenorhabditis elegans* chemotaxis. J. Neurosci. *19*, 9557–9569.

Pierce-Shimomura, J.T., Chen, B.L., Mun, J.J., Ho, R., Sarkis, R., and McIntire, S.L. (2008). Genetic analysis of crawling and swimming locomotory patterns in *C. elegans*. Proc. Natl. Acad. Sci. USA *105*, 20982–20987.

Pirri, J.K., McPherson, A.D., Donnelly, J.L., Francis, M.M., and Alkema, M.J. (2009). A tyramine-gated chloride channel coordinates distinct motor programs of a *Caenorhabditis elegans* escape response. Neuron *62*, 526–538.

Rela, L., and Szczupak, L. (2004). Gap junctions: their importance for the dynamics of neural circuits. Mol. Neurobiol. *30*, 341–357.

Starich, T.A., Herman, R.K., and Shaw, J.E. (1993). Molecular and genetic analysis of unc-7, a *Caenorhabditis elegans* gene required for coordinated locomotion. Genetics *133*, 527–541.

Starich, T.A., Xu, J., Skerrett, I.M., Nicholson, B.J., and Shaw, J.E. (2009). Interactions between innexins UNC-7 and UNC-9 mediate electrical synapse specificity in the *Caenorhabditis elegans* locomotory nervous system. Neural Dev. *4*, 16.

Stirman, J.N., Crane, M.M., Husson, S.J., Wabnig, S., Schultheis, C., Gottschalk, A., and Lu, H. (2011). Real-time multimodal optical control of neurons and muscles in freely behaving *Caenorhabditis elegans*. Nat. Methods *8*, 153–158.

White, J.G., Southgate, E., Thomson, J.N., and Brenner, S. (1976). The structure of the ventral nerve cord of *Caenorhabditis elegans*. Philos. Trans. R. Soc. Lond. B Biol. Sci. *275*, 327–348.

Wicks, S.R., Roehrig, C.J., and Rankin, C.H. (1996). A dynamic network simulation of the nematode tap withdrawal circuit: predictions concerning synaptic function using behavioral criteria. J. Neurosci. *16*, 4017–4031.

Yeh, E., Kawano, T., Ng, S., Fetter, R., Hung, W., Wang, Y., and Zhen, M. (2009). *Caenorhabditis elegans* innexins regulate active zone differentiation. J. Neurosci. *29*, 5207–5217.

Zhang, Y., Narayan, S., Geiman, E., Lanuza, G.M., Velasquez, T., Shanks, B., Akay, T., Dyck, J., Pearson, K., Gosgnach, S., et al. (2008). V3 spinal neurons establish a robust and balanced locomotor rhythm during walking. Neuron *60*, 84–96.

Zheng, Y., Brockie, P.J., Mellem, J.E., Madsen, D.M., and Maricq, A.V. (1999). Neuronal control of locomotion in *C. elegans* is modified by a dominant mutation in the GLR-1 ionotropic glutamate receptor. Neuron *24*, 347–361.